DETERMINATION OF THE THERMAL-HYDRAULIC PARAMETERS OF I.T.U. TRIGA MARK-II REACTOR

Ahmet DURMAYAZ*, Emin Hakan ÖZKUL**

Institute for Nuclear Energy, Istanbul Technical University, Maslak, TR-80626, Istanbul, TÜRKIYE

ABSTRACT

In this study, a transient, one-dimensional thermal-hydraulic subchannel analysis for I.T.U. TRIGA Mark-II reactor was employed. Mixed convection is considered in modelling to enhance the capability of the computer code. After the continuity, conservation of energy, momentum balance equations for coolant in axial direction and the heat-conduction equation for the fuel rod in radial direction had been written, they were discretized by using the control volume approach to obtain a set of algebraic equations. By the aid of the discretized continuity and momentum balance equations, a pressure and a pressure-correction equations were derived. Then, two different FORTRAN programs called **TRIGATH** (**TRIGA** Thermal-**H**ydraulics) and **TRIGATH-R** (**TRIGATH R**evised) have been developed to solve this set of algebraic equations by using SIMPLE and SIMPLER algorithms respectively. As a result, the temperature distributions of the coolant and the fuel rods as well as the velocity and pressure distributions of the coolant have been estimated for both transient and steady state regimes from both algorithms. Their results, which are in good agreement, are compared to the results of the computer code TRISTAN.

1. INTRODUCTION

The I.T.U. TRIGA Mark-II reactor has been operated in two modes: steady-state and pulsing. Reactor power levels in steady-state mode range up to and include 250 kW. Maximum power in transient pulsing mode reaches up to approximately 1200 MW [1,2]. The reactor core assembly shown in Fig. 1 is located near the bottom of a cylindrical aluminum tank surrounded by a reinforced concrete shield structure. The reactor is equipped with a central thimble for conducting experiments or irradiating small samples in the core, a pneumatic transfer system for production of short-lived radioisotopes. The biological shield is pierced by three beam tubes and the thermal column for irradiation purposes.

The core consists of ninety vertical cylindrical elements located in five rings around the central thimble. Sixty-nine of them are fuel elements, which consist of four components: (1) fuel-moderator meat, (2) graphite reflectors, (3) cladding, (4) end fixtures. Fuel elements are spaced in the core by means of aluminum top and bottom grid plates. The bottom grid plate has spaces to permit coolant passage through the plate. The safety analysis of I.T.U. TRIGA Mark–II reactor requires a thermal-

* Assoc. Prof. Dr., Corresponding author. Tel.: +90 (212) 285 3946; Fax: +90 (212) 285 3884; e-mail: durmayaz@itu.edu.tr
** M.Sc.

hydraulic model of the reactor to determine the thermal-hydraulic parameters in both steady-state and transient mode operations.

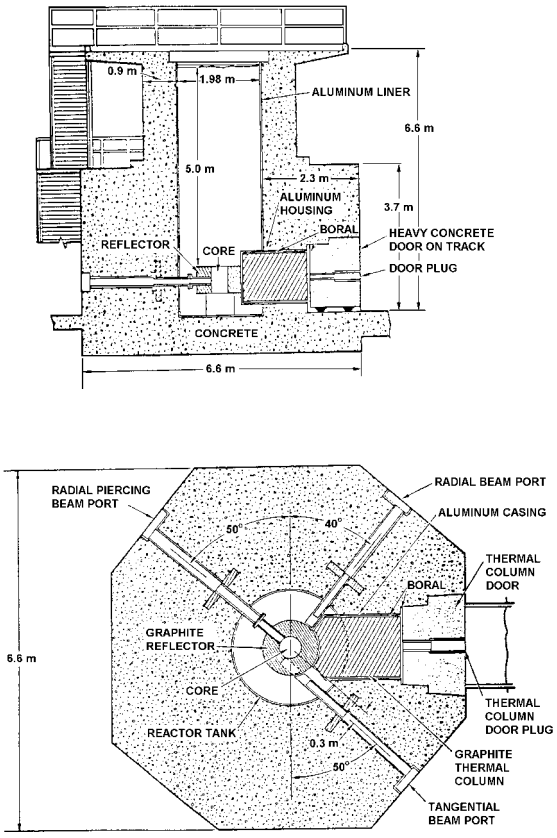

Figure 1. I.T.U. TRIGA Mark-II reactor arrangement [1,2].

2. THE THERMAL-HYDRAULIC MODEL

The reactor has been operated with natural convective cooling by pool water, which is also cooled and purified in external coolant circuits by forced convection. In this study, therefore, this characteristic cooling system of the tank water leads to consider "**mixed convection**", which is based on both natural and forced convection, in a "**subchannel analysis**", in which the properties of coolant are represented by single area-averaged values for each subchannel. In general, the subchannel analysis method uses either the coolant-centered or the rod-centered subchannel approaches. The traditional approach for rod bundle analysis has been coolant-centered subchannels. However, **"the rod-centered subchannel"** approach shown in Fig. 2 is considered in this study since it provides a regular, well-arranged geometry. In this way, the thermal-hydraulic parameters are easily calculated in these rod-centered subchannels [3,4]. Each subchannel in I.T.U. TRIGA Mark-II reactor core is called by the same name of the rod it

contains in this analysis. The flow area of any subchannel is the z-directional cross-sectional area filled by the fluid. The hydraulic diameter of a subchannel is the equivalent diameter of the flow area in the subchannel. The fuel rod has an outer radius of 1.8669 cm and its active fuel meat section has a height of 38.1 cm.

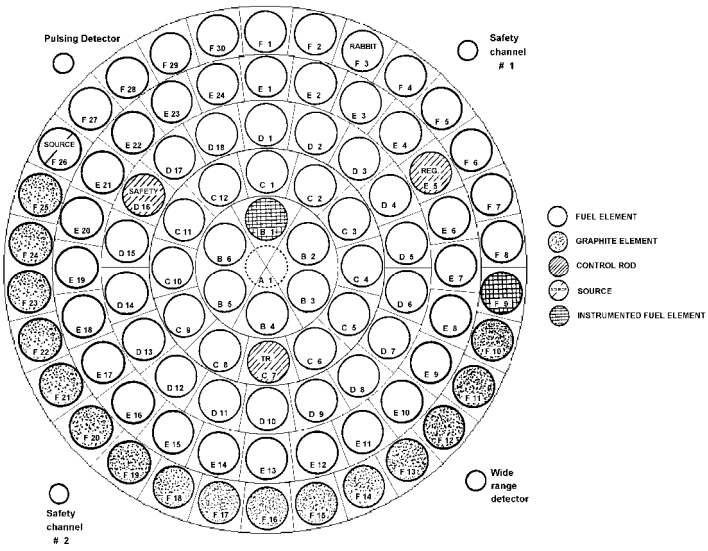

Figure 2. The rod-centered subchannels on I.T.U. TRIGA Mark-II reactor core.

The "**assumptions**" of this thermal-hydraulic model are as follows [3,4]:

1-There is no mass, momentum or energy transfer between the subchannels in r- and θ -directions.

2- The heat transfer from the fuel to the top and bottom graphite reflectors in z-direction is ignored.

3- Each property of the coolant has a uniform distribution in r- and θ -directions in a subchannel.

4- Energy is produced homogeneously on the horizontal cross-section of a fuel.

5- The reactor works either in transient or in steady-state mode.

6- The core inlet temperature and velocity do not change in time.

7- The density ρ, dynamic viscosity μ, specific heat c_p and conductivity k of the coolant are functions of temperature and pressure. These parameters and the Prandtl number Pr have been calculated by means of the computer program H2O [5].

8- The thermal conductivity k_f and the specific heat c_f of the fuel and the thermal conductivity k_{cl} of the clad are temperature-dependent. They are calculated from the following correlations [6]:

$$k_f = \frac{0.17585}{1 - 4.15\times10^{-4}\,T_f} \quad \text{(W/m K)}, \tag{1}$$

$$k_{cl} = \frac{13.4634}{1 - 9.6884\times10^{-4}\,T_{cl}} \quad \text{(W/m K)}, \tag{2}$$

$$c_f = 857 + 1.6\,(T_f - 25) \quad \text{(kJ/kg K)}. \tag{3}$$

9- The constant values of c_{cl}=460 (kJ/kg K), ρ_f=6000 (kg/m^3) and ρ_{cl}=7865 (kg/m^3) are considered for the fuel and clad.

10- The free convection heat transfer coefficient h is calculated from the following correlations, which are given for the outside surface of a vertical cylinder [6-9]:

a) Laminar flow

$$h = 0.59\,k(Gr\,Pr)^{0.25}/H \quad \text{for} \quad 10^4 \le Gr\,Pr \le 10^9, \tag{4}$$

Turbulent flow

$$h = 0.10(Gr\,Pr)^{1/3}/H \quad \text{for} \quad 10^9 \le Gr\,Pr \le 10^{13} \tag{5}$$

where H is the length. Grashoff number is also defined as

$$Gr = \frac{g\beta\rho^2}{\mu^2}(T_{cl} - T)H^3. \tag{6}$$

3. GOVERNING DIFFERENTIAL EQUATIONS

In this study, the aim is to constitute a "**one-dimensional**" thermal-hydraulic model having all dependent variables "**area-averaged**". Three-dimensional continuity, momentum balance and conservation of energy equations in cylindrical coordinates for the coolant have been written easily by the aid of [10-14]. As the detailed information is given in [3], after integrating these equations over the cross-sectional flow area perpendicular to the z- (flow) direction, the area-averaged one-dimensional continuity, momentum balance and conservation of energy equations for the coolant in cylindrical coordinates are obtained as follows:

One-Dimensional Continuity Equation

$$\frac{\partial\rho}{\partial t} + \frac{\partial(\rho v_z)}{\partial z} = 0, \tag{7}$$

One-Dimensional Conservation of Energy Equation

$$\frac{\partial(\rho T)}{\partial t}+\frac{\partial(\rho v_z T)}{\partial z}=\frac{k}{c_p}\left(\frac{\partial^2 T}{\partial z^2}\right)+\frac{q'''}{c_p}, \tag{8}$$

One-Dimensional Momentum Balance Equation

$$\frac{\partial(\rho v_z)}{\partial t}A_{z-s}+\frac{\partial(\rho v_z v_z)}{\partial z}A_{z-s}=-\frac{\partial p_d}{\partial z}A_{z-s}+\mu\frac{\partial^2 v_z}{\partial z^2}A_{z-s}-\tau P-\rho g\beta(T-T_0)A_{z-s} \tag{9}$$

where v_z is the z-directional velocity component of the coolant, p_d is the dynamic pressure, τ is the shear stress and P is the perimeter. Shear stress can be written as

$$\tau=0.5\rho v_z|v_z|f \tag{10}$$

while f is the friction factor, which is given [11] for laminar flow and round tube as

$$f=\frac{16}{Re_{D_H}} \tag{11}$$

where Re_{D_H} is the Reynolds number considering the hydraulic diameter. In the derivation of the momentum equation, the total pressure that expresses the absolute pressure is divided into three parts: atmospheric, dynamic and hydraustatic pressures. Since the z-directional change in the atmospheric pressure is zero, the term related to it is dropped. It is assumed that *the density of the fluid in the buoyancy (last) term of Eq. (9) is variable, while the density in the other terms are constant*. This assumption is known as the ***Boussinesq Approach***.

4. GRID STRUCTURE

Grid for the continuity, the conservation of energy, the pressure and the pressure correction equations is shown in Fig. 3a and staggered grid for the momentum balance equation is shown in Fig. 3b [3,4,15]. In Fig. 3a, shaded area is a control volume denoted by point P. Points W and E also denote the neighbor control volumes while w and e denote the interfaces between the two neighbor control volumes.

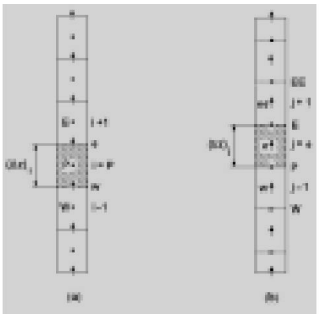

Figure 3. Grid (a) for the continuity, the conservation of energy, the pressure and the pressure correction equations and, staggered grid (b) for the momentum balance equation.

To derive a set of discretized algebraic equations with the help of the **"control volume approach"**, the differential equations given by Eqs. (7)-(9) are integrated over the control volumes shown in Fig. 3. During the integration process, a **"fully implicit hybrid scheme"** is used, so that the values of temperature, velocity and pressure at time $t+\Delta t$ are assumed to prevail over the entire time step [3,4,15,16].

5. DISCRETIZATION EQUATIONS FOR THE CONSERVATION Of ENERGY EQUATION

After integrating Eq. (8) over the control volume shown in Fig. 3a, the final form of the *discretized conservation of energy equation* for hybrid scheme is obtained [3,4] as

$$a_P^T T_P = a_E^T T_E + a_W^T T_W + b^T \tag{12}$$

where

$$a_E^T = \left\| -F_e^T, 0 \right\| + D_e^T \left\| 1 - \frac{\left| F_e^T \right|}{2D_e^T}, 0 \right\|, \tag{13}$$

$$a_W^T = \left\| F_w^T, 0 \right\| + D_w^T \left\| 1 - \frac{\left| F_w^T \right|}{2D_w^T}, 0 \right\|, \tag{14}$$

$$\left(a_P^T\right)^0 = \frac{\rho_P^0 (\Delta z)_P (A_{z-s})_P}{\Delta t}, \tag{15}$$

$$b^T = \left(S_c^T\right)_P (\Delta z)_P (A_{z-s})_P + \left(a_P^T\right)^0 T_P{}^0, \tag{16}$$

$$a_P^T = a_E^T + a_W^T + \left(a_P^T\right)^0 - \left(S_p^T\right)_P (\Delta z)_P (A_{z-s})_P . \tag{17}$$

The name **"hybrid scheme"** is the indicative of a combination of the **central difference** and **upwind schemes**. An automatic selection of scheme is provided by the symbol of $\|A, B\|$, which has a meaning of "*choose the largest of A and B*", given in Eqs. (13) and (14). The value of the Peclet number is compared to choose either the central difference or the upwind scheme in the hybrid scheme to employ. The criteria is that the hybrid scheme applies the upwind method while

$$|P| > 2 \tag{18}$$

and it applies the central difference method while

$$|P| < 2 \tag{19}$$

where P is a Peclet number, which is defined by

$$P \equiv \frac{F^T}{D^T}. \tag{20}$$

6. DISCRETIZATION EQUATIONS FOR THE MOMENTUM BALANCE EQUATION

After integrating Eq. (9) over the control volume shown in Fig. 3b, the *discretized momentum balance equation* for the hybrid scheme is obtained [3,4] as

$$a_e^v (v_z)_e = a_{ee}^v (v_z)_{ee} + a_w^v (v_z)_w + b^v + (p_P - p_E)(A_{z-s})_e \tag{21}$$

where

$$a_{ee}^v = \|-F_E, 0\| + D_E \left\| 1 - \frac{1}{2}\left|\frac{F_E}{D_E}\right|, 0 \right\|, \tag{22}$$

$$a_w^v = \|F_P, 0\| + D_P \left\| 1 - \frac{1}{2}\left|\frac{F_P}{D_P}\right|, 0 \right\|, \tag{23}$$

$$\left(a_e^v\right)^0 = \frac{\left(\rho^0\right)_e (\delta z)_e (A_{z-s})_e}{\Delta t}, \tag{24}$$

$$b^v = \left(S_c^v\right)_e (\delta z)_e (A_{z-s})_e + \left(a_P^v\right)^0 (v_z)_e^0, \tag{25}$$

$$a_e^v = a_{ee}^v + a_w^v + \left(a_e^v\right)^0 - \left(S_p^v A_{fr}\right)_e \tag{26}$$

while

$$\left(S_c^v\right)_e = \rho g \beta (T_e - T_0), \tag{27}$$

$$\left(S_p^v\right)_e = -\frac{1}{2}\left(\rho |v_z| f\right)_e . \tag{28}$$

7. THE PRESSURE-CORRECTION EQUATION

The momentum balance equation can be solved only when the pressure field is given or somehow estimated. For this aim, a pressure-correction equation to give the error p' on the guessed pressure field p^* for obtaining the correct pressure field p is derived [3,4]. During the derivation, the correct pressure p is proposed to be obtained as

$$p = p^* + p' \tag{29}$$

where p' is called the *pressure-correction*. A *velocity-correction formula* can also be obtained as

$$(v_z)_e \cong \left(v_z^*\right)_e + d_e \left(p_P' - p_E'\right) \tag{30}$$

from the discretized momentum balance equation. One can substitute the velocity-correction formula into the discretized continuity equation and rearrange it to obtain the *pressure-correction equation* as

$$a_P^{p'} p'_P = a_E^{p'} p'_E + a_W^{p'} p'_W + b^{p'} \tag{31}$$

where

$$a_E^{p'} = (\rho d A_{z-s})_e, \tag{32}$$

$$a_W^{p'} = (\rho d A_{z-s})_w, \tag{33}$$

$$a_P^{p'} = a_E^{p'} + a_W^{p'}, \tag{34}$$

$$b^{p'} = \frac{(\rho^0 - \rho)_P}{\Delta t}(\Delta z)_P (A_{z-s})_P + \left[(\rho v_z^*)_w - (\rho v_z^*)_e\right](A_{z-s})_P = 0. \tag{35}$$

8. DERIVATION Of THE PRESSURE EQUATION

An equation to obtain the pressure field can be derived as follows [15,16]. The *momentum balance equation*, Eq.(21), in discretized form is rewritten as

$$v_e = \frac{a_{ee}^v v_{ee} + a_w^v v_v + b^v}{a_e^v} + d_e (p_P - p_E) \tag{36}$$

where

$$d_e = \frac{(A_{z-s})_e}{a_e^v}. \tag{37}$$

Now, we define a *pseudovelocity* $\hat{v}_e$ by

$$\hat{v}_e = \frac{\sum a_{nb}^v v_{nb} + b^v}{a_e^v}. \tag{38}$$

As it is shown, $\hat{v}_e$ is composed of the neighbor velocities v_{nb} and contains no pressure. Thus, Eq. (36) becomes

$$v_e = \hat{v}_e + d_e (p_P - p_E). \tag{39}$$

Similarly,

$$v_w = \hat{v}_w + d_w (p_W - p_P) \tag{40}$$

can be written. Employing the fully implicit method, the integration of Eq. (7) over the control volume shown in Fig. 3a gives the *discretized continuity equation* as

$$\frac{(\rho - \rho^0)_P}{\partial t}(\Delta z)_P (A_{z-s})_P + \left[(\rho v_z)_e - (\rho v_z)_w\right](A_{z-s})_P = 0. \tag{41}$$

One can substitute Eqs. (39) and (40), into Eq. (41) and rearrange it to obtain the *pressure equation* in discretized form as

$$a_P^p\ p_P = a_E^p\ p_E + a_W^p\ p_W + b^p \tag{42}$$

where

$$a_E^p = (\rho d A_{z-s})_e, \tag{43}$$

$$a_W^p = (\rho d A_{z-s})_w, \tag{44}$$

$$a_P^p = a_E^p + a_W^p, \tag{45}$$

$$b^p = \frac{(\rho^0 - \rho)_P}{\Delta t}(\Delta z)_P (A_{z-s})_P + [(\rho \hat{v}_z)_w - (\rho \hat{v}_z)_e](A_{z-s})_P = 0. \tag{46}$$

9. NUMERICAL SOLUTION PROCEDURE: SIMPLE AND SIMPLER ALGORITHMS

The procedure used in the calculation of the flow field together with the pressure and temperature fields has been given the name **SIMPLE**, which stands for **S**emi-**I**mplicit **M**ethod for **P**ressure-**L**inked **E**quation [15,16]. The important operations for the execution of this algorithm are summarized in the flow chart shown in Fig. 4a. To improve the rate of convergence of **SIMPLE** algorithm, a revised version has also been worked out. It is called **SIMPLER** which stands for **SIMPLE R**evised [15,16]. It consists of solving the pressure equation to obtain the pressure field and solving the pressure-correction equation only to correct the velocities. The operations for the execution of this algorithm are shown in the flow chart in Fig. 4b.

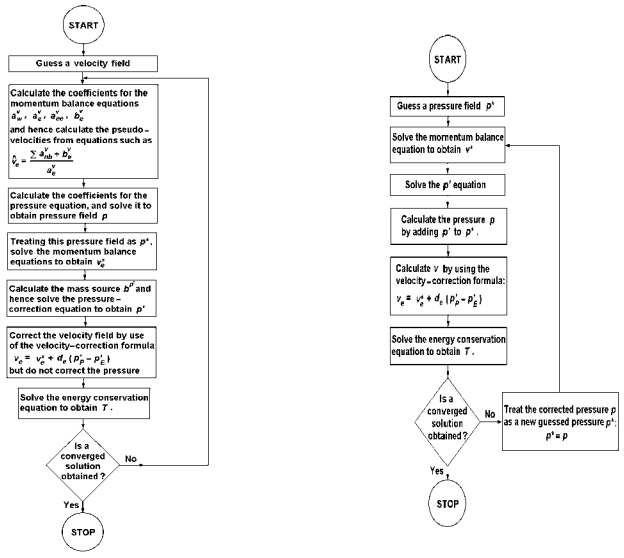

(a) **(b)**

Figure 4. (a) The SIMPLE and (b) the SIMPLER algorithms.

The set of boundary conditions used in this model is that velocity and temperature are specified at the inflow boundary whereas pressure is specified at the outflow boundary.

The solution of the discretization equations for one-dimensional situation is obtained by the standard "**Gauss-elimination method**", which is sometimes called the "**Thomas Algorithm**" or the "**TDMA**" (**T**ri**D**iagonal **M**atrix **A**lgorithm).

10. THE HEAT-CONDUCTION EQUATION FOR THE FUEL RODS

One-dimensional heat-conduction equation for the fuel rods in cylindrical coordinates can be written [17] as

$$\frac{\partial(\rho c_v T)}{\partial t} = \frac{1}{r}\frac{\partial}{\partial r}\left(kr\frac{\partial T}{\partial r}\right) + q''' . \tag{47}$$

One can obtain a discretization equation for the heat-conduction equation [3,4,15] as

$$a_P^T T_P = a_S^T T_S + a_N^T T_N + b^T \tag{48}$$

where subscripts S and N denote the neighbor control volumes in radial direction and

$$a_S^T = \frac{r_s k_s}{(\delta r)_s}, \tag{49}$$

$$a_N^T = \frac{r_n k_n}{(\delta r)_n}, \tag{50}$$

$$\left(a_P^T\right)^0 = \frac{(\rho c_v)_P}{\Delta t}\left(\frac{r_s + r_n}{2}\right)(\Delta r)_P , \tag{51}$$

$$b^T = \left(S_c^T\right)_P\left(\frac{r_s + r_n}{2}\right)(\Delta r)_P + \left(a_P^T\right)^0 T_P{}^0 , \tag{52}$$

$$a_P^T = a_S^T + a_N^T + \left(a_P^T\right)^0 - \left(S_p^T\right)_P\left(\frac{r_s + r_n}{2}\right)(\Delta r)_P . \tag{53}$$

11. COMPUTATIONAL RESULTS

After the development of the thermal-hydraulic model, two different FORTRAN programs called **TRIGATH** (**TRIGA** Thermal-**H**ydraulics) [3,4] and **TRIGATH-R** (**TRIGATH** **R**evised) that employ SIMPLE and SIMPLER algorithms respectively have been coded. A cosine linear power density variation in z-direction is considered in all runs of both computer codes. In the sample runs of the codes to obtain the results given below, coolant temperature and velocity are assumed to be $32.5\,^{o}\mathrm{C}$ and 0.1201 m/s respectively as both the initial and the inlet boundary conditions. Dynamic pressure is assumed to be 1×10^{-7} Pa at the outlet of reactor core. The fuel element thermal powers of different fuel rods that correspond to a

maximum steady reactor power of 250 kW, grid structure in radial direction, some thermophysical properties of the fuel element B1 and some thermophysical parameters of the coolant used in the thermal-hydraulic model of I.T.U. TRIGA Mark-II reactor are presented in [3,4]. Similar results are obtained from the run of both TRIGATH and TRIGATH-R codes.

Axial directional variation of some thermal-hydraulic parameters in subchannel B1 at a maximum steady power of 250 kW of I.T.U. TRIGA Mark-II reactor are presented in Table 1.

Table 1. Axial directional variation of some thermal-hydraulic parameters of the coolant and fuel rod in subchannel B1 for I.T.U. TRIGA Mark-II reactor.

Zone	z_{in} (cm)	z_{out} (cm)	Absolute pressure (Pa)	Hydraustatic pressure (Pa)	Velocity (m/s)	Temperature (°C)	T_{cl} (°C)	$T_{f\,outer}$ (°C)	$T_{f\,center}$ (°C)
15	16,51	19,05	151326,85	50001,85	12,074	46,50	109,15	111,88	144,58
14	13,97	16,51	151573,66	50249,77	12,072	45,93	121,20	124,58	165,29
13	11,43	13,97	151820,53	50497,70	12,068	45,21	131,40	135,35	183,07
12	8,89	11,43	152067,47	50745,62	12,064	44,36	139,75	144,17	197,80
11	6,35	8,89	152314,49	50993,55	12,059	43,40	146,21	151,00	209,33
10	3,81	6,35	152561,60	51241,48	12,054	42,35	150,72	155,78	217,53
9	1,27	3,81	152808,80	51489,40	12,048	41,24	153,25	158,47	222,29
8	-1,27	1,27	153056,11	51737,33	12,043	40,08	153,74	159,02	223,55
7	-3,81	-1,27	153303,51	51985,25	12,037	38,92	152,17	157,40	221,26
6	-6,35	-3,81	153551,02	52233,18	12,032	37,76	148,53	153,60	215,41
5	-8,89	-6,35	153798,63	52481,10	12,027	36,65	142,83	147,63	206,05
4	11,43	-8,89	154046,33	52729,03	12,023	35,60	135,07	139,51	193,25
3	13,97	-11,43	154294,12	52976,95	12,019	34,64	125,30	129,27	177,13
2	16,51	-13,97	154541,99	53224,88	12,015	33,79	113,57	116,97	157,82
1	19,05	-16,51	154789,93	53472,80	12,012	33,07	99,88	102,64	135,47

Variations of the steady-state axial fuel temperature distributions at the fuel rod center in different rings at a maximum steady power of 250 kW of reactor are plotted in Fig. 5.

Variations of the steady state radial temperature distribution in the fuel rods of different rings at a maximum steady power of 250 kW of reactor are also plotted in Fig. 6.

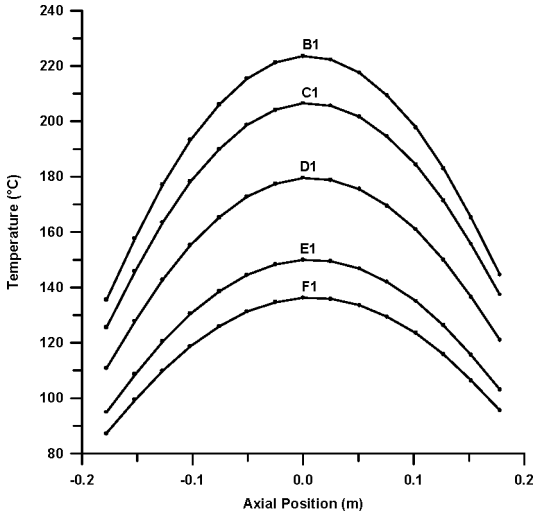

Figure 5. Variations of the steady state axial fuel temperature distributions at the fuel rod center in different rings.

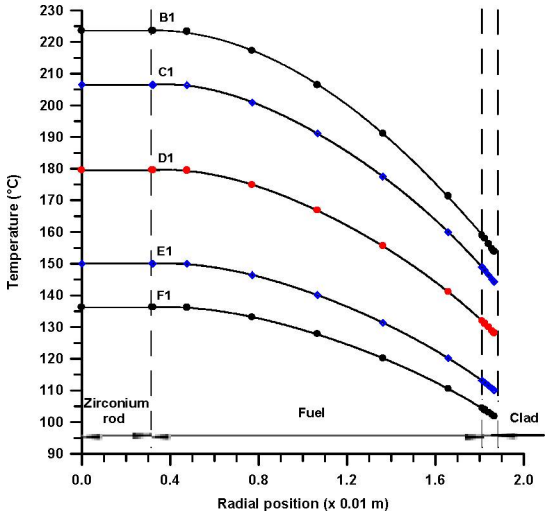

Figure 6. Variations of the steady state radial temperature distribution in the fuel rods of different rings.

The data for the coolant of I.T.U. TRIGA Mark-II reactor obtained from the run of TRISTAN are presented in Table 2 to compare the results of this study and TRISTAN [18,19]. The data, which is the estimations for maximum temperatures at the outer surface of clad, at the

outer surface and in the center of fuel in radial direction obtained from the run of TRISTAN for I.T.U. TRIGA Mark-II reactor, is given in the second-fourth columns of Table 3 [18,19]. The data given in the last column of Table 3 is the result of measurements for the maximum temperatures nearly in the center of fuels at different rings of I.T.U. TRIGA Mark-II reactor [19], which are given for a comparison.

Table 2. Some of the thermal-hydraulic parameters obtained from the run of TRISTAN for the coolant of I.T.U. TRIGA Mark-II reactor [18,19].

Zone	Height (cm)	Temperature (°C)	Hydraustatic Pressure Drop (Pa)	Density (kg/m^3)	Velocity (cm/s)
15	52,36	46,43	245,73	0,9886	12,07
14	49,82	45,76	245,57	0,9899	12,07
13	47,28	44,95	245,49	0,9902	12,06
12	44,74	44,01	245,13	0,9906	12,06
11	42,20	42,97	245,22	0,9910	12,05
10	39,66	41,84	245,38	0,9914	12,05
9	37,12	40,67	245,59	0,9919	12,04
8	34,58	39,47	245,84	0,9923	12,04
7	32,04	38,26	246,12	0,9928	12,03
6	29,50	37,09	246,40	0,9932	12,03
5	26,96	35,97	246,69	0,9937	12,02
4	24,42	34,92	247,31	0,9940	12,02
3	21,88	33,98	247,64	0,9944	12,01
2	19,33	33,17	247,87	0,9947	12,01
1	16,80	32,50	248,07	0,9950	12,01

Table 3. Maximum temperatures obtained from the run of TRISTAN [18,19] and measured experimentally in the fuel rods in different rings of I.T.U. TRIGA Mark-II reactor [19].

Position	T_{cl} (°C)	T_f (°C)	$T_{f\,max}$ (°C)	$T_{f\,max,exp}$ (°C)
B1	133	141	256	244
C1	126	134	230	219
D1	123	127	213	204
E1	113	118	183	176
F1	88	91	147	141

12. CONCLUSIONS

In this study, a transient, one-dimensional thermal-hydraulic subchannel analysis for I.T.U. TRIGA Mark-II reactor has been employed. The temperature, pressure and velocity distributions for the coolant in axial direction together with the temperature distribution of the fuel rods in radial direction for I.T.U. TRIGA Mark-II reactor have been estimated for both transient and steady states by the computer code TRIGATH-R developed during this study. The data used in TRIGATH-R are the same, in majority, as those of TRISTAN. Although TRIGATH-R considers rod-centered subchannels while TRISTAN considers triangular subchannels, their estimations for the hydraustatic pressure drops, velocity, and temperature gradients given in Table 1 are in good agreement with those of TRISTAN given in Table 2 [18,19]. The convergence of the code TRIGATH-R is also perfect.

REFERENCES

[1] Safety Analysis Report for the TRIGA Mark-II Reactor for the Institute for Nuclear Energy, Technical University of Istanbul, Turkey, 1978.

[2] TRIGA Mark-II Reactor Mechanical Operation and Maintenance Manual, GA Project 2129, March 1, 1978.

[3] ÖZKUL, E.H. Thermal-hydraulic Analysis of I.T.U. TRIGA Mark-II Reactor, M.Sc. Thesis, I.T.U. Institute for Nuclear Energy, June 2000.

[4] ÖZKUL, E.H., DURMAYAZ, A., A Parametric Thermal-hydraulic Analysis of I.T.U. TRIGA Mark-II Reactor, 16th TRIGA Conference, Institute for Nuclear Research, Pitesti, Romania, Sep. 25-28, 2000.

[5] H2O, Calculation of Thermodynamic Properties of Steam and H2O, OECD Nuclear Energy Agency Databank, NEA 0876 0984.

[6] CAN, B., YAVUZ, H., AKBAY, E., The Investigation of Nonlinear Dynamics Behavior of I.T.U. TRIGA Mark-II Reactor, Eleventh European TRIGA Users Conference, Heidelberg, Germany, 2.39-2.49 Sep.11-13, 1990.

[7] CAN, B., YAVUZ, H., I.T.Ü. TRIGA Mark-II Reaktörünün Nonlineer Simülasyonu, Yöneylem Arastirmasi ve Endüstri Mühendisligi 91. Ulusal Kongresi, I.T.Ü. Istanbul, 17-19 Haziran 1991.

[8] CAN, B., YAVUZ, H., I.T.Ü. TRIGA Mark-II Reaktörü Termo-Hidrolik Analizi, Marmara Üniversitesi Fen Bilimleri Dergisi, Sayi 2, Say.229-237, Istanbul, 1985.

[9] CAN, B., KURUL, N., BÜKE, T., YAVUZ, H., I.T.Ü. TRIGA Mark-II Reaktörünün Dinamik Davranisi, 5. Ulusal Nükleer Bilimler Kongresi, Dokuz Eylül Üniversitesi Nükleer Bilimler Enstitüsü Izmir, 22-24 Mayıs 1991.

[10] TODREAS, N.E., KAZIMI, M.S., Nuclear Systems II, Elements of Thermal Hydraulic Design, Hemisphere Publishing Corp., 1990.

[11] BEJAN, A, Convection Heat Transfer, John Wiley and Sons, 1984.

[12] ARPACI, V., LARSEN, P.S., Convection Heat Transfer, Prentice-Hall Inc., 1984.

[13] WALLIS, G.B., One-Dimensional Two-Phase Flow, Mc Graw-Hill Book Company, 1969.

[14] SERTELLER, G., Nükleer Yakıt Sogutucu Kanallarında Birleşik Tasinimla Isı Transferinin Sayisal Çözümü, Yüksek Lisans Tezi, I.T.Ü. Nükleer Enerji Enstitüsü, 1997.

[15] PATANKAR, S.V., Numerical Heat Transfer and Fluid Flow, Hemisphere Publishing Corporation, 1980.

[16] PATANKAR, S.V., SPALDING, D.B., A Calculation Procedure for Heat, Mass and Momentum Transfer in Three-Dimensional Parabolic Flows, Int. J. of Heat and Mass Transfer, Vol. 15, pp.1787-1806, 1972.

[17] HOLMAN, J.P., Heat Transfer, McGraw-Hill Book Company, 1989.

[18] MELE, I., ZEFRAN, B., TRISTAN: A Computer Program for Calculating Natural Convection Flow Parameters in TRIGA Core, University of Ljubljana, Slovenia, 1992.

[19] BÜKE, T., YAVUZ, H., Thermal-Hydraulic Analysis of the I.T.U. TRIGA Mark-II Reactor, 1st Eurasia Conference on Nuclear Science and Its Application, Izmir- Turkiye, 23-27 Oct. 2000.